Original Article

Gray matter alterations in tremor-dominant Parkinson's disease after MRgFUS thalamotomy are correlated with tremor improvement: a pilot study

Xiaoyu Wang[1,2#], Song Wang[1#], Jiaji Lin[1#], Dong Zhang[1], Haoxuan Lu[1], Yongqin Xiong[1], Linlin Deng[1], Dekang Zhang[1], Xiangbing Bian[1], Jiayou Zhou[3], Longsheng Pan[3*], Xin Lou[1,2*^]

[1]Department of Radiology, Chinese PLA General Hospital, Beijing, China; [2]School of Medicine, Nankai University, Tianjin, China; [3]Department of Neurosurgery, Chinese PLA General Hospital, Beijing, China

Contributions: (I) Conception and design: X Wang, S Wang, J Lin; (II) Administrative support: X Lou, L Pan; (III) Provision of study materials or patients: All authors; (IV) Collection and assembly of data: All authors; (V) Data analysis and interpretation: All authors; (VI) Manuscript writing: All authors; (VII) Final approval of manuscript: All authors.

[#]These authors contributed equally to this work.

[*]These authors are shared corresponding authors.

Correspondence to: Xin Lou, MD. Department of Radiology, Chinese PLA General Hospital, 28 Fuxing Road, Beijing 100853, China. Email: louxin@301hospital.com.cn; Longsheng Pan, MD. Department of Neurosurgery, Chinese PLA General Hospital, 28 Fuxing Road, Beijing 100853, China. Email: panls301@163.com.

Background: Regional differences in gray matter volume (GMV) have been reported to be a reliable marker for diagnosing Parkinson's disease (PD). This study aimed to explore the clinical value of GMV to assess magnetic resonance imaging-guided focused ultrasound (MRgFUS) thalamotomy as a treatment for tremor-dominant PD (TDPD).

Methods: Nine TDPD patients with MRgFUS thalamotomy were recruited for structural magnetic resonance image (MRI) scanning and clinical score evaluation. GMV was calculated. To investigate changes after treatment, voxel- and region of interest (ROI)-wise GMV analyses were performed. Then, GMV with significant differences was extracted from patients to investigate its dynamic alterations by one-way repeated-measures analysis of variance (ANOVA). The nonparametric Spearman rank correlation analysis was used to evaluate the relationship between GMV alterations and tremor improvement after thalamotomy.

Results: Tremors were significantly relieved after MRgFUS thalamotomy in nine patients ($P<0.05$). The treated hand tremor scores improved 74.82% on average in patients from pre-operation to 12 months post-operation. Voxel-wise analysis at the cluster level showed a significant decrease in GMV in the left middle occipital gyrus (MOG) [$t=11.81$, voxel-level $P<0.001$, cluster-level $P_{\text{family-wise error (FWE)}}<0.05$] and an increase in GMV in the left precentral gyrus (PreCG) ($t=7.99$, voxel-level $P<0.001$, cluster-level $P_{FWE}<0.05$) in TDPD patients from preoperative to 12 months post-operation, which was significantly correlated with tremor scores (rho =0.346–0.439, $P<0.05$). ROI-wise analysis showed that GMV related to MRgFUS thalamotomy was associated with long-term structural alterations ($P<0.05$ with Bonferroni correction), including specific basal ganglia and related nuclei and cerebellum subregions.

^ ORCID: 0000-0003-2980-5171.

Conclusions: GMV can be used to reflect tremor improvement after MRgFUS thalamotomy and be helpful to better understand the distant effect of MRgFUS thalamotomy and the involvement of GMV in tremor control in TDPD.

Trial Registration: ClinicalTrials.gov identifier: NCT04570046.

Keywords: Tremor-dominant Parkinson's disease; magnetic resonance imaging-guided focused ultrasound (MRgFUS); voxel-based morphometry (VBM); gray matter; cerebellum

Submitted Dec 18, 2022. Accepted for publication Apr 17, 2023. Published online May 04, 2023.
doi: 10.21037/qims-22-1403
View this article at: https://dx.doi.org/10.21037/qims-22-1403

Introduction

Tremor-dominant Parkinson's disease (TDPD) is a clinical subtype with characteristics distinct from akinesia, rigidity, postural instability, and gait disorder subtypes (1). Tremor, as one of the cardinal symptoms, is present in more than 70% of patients during their progression of the disease (2). The pathophysiology of tremor has been related to the combined actions of both the basal ganglia and the cerebello-thalamo-cortical (CTC) circuit (3,4). Compared with other subtypes, TDPD may be more resistant to drug therapy than bradykinesia or rigidity. For these patients, functional neurosurgery is used to improve the symptoms of patients, such as magnetic resonance imaging-guided focused ultrasound (MRgFUS), deep brain stimulation, and radiofrequency ablation (5-7).

MRgFUS thalamotomy could relieve at least 65% of tremors in Parkinson's disease (PD) by using high-intensity ultrasound energy to ablate the ventral intermediate (VIM) nucleus (7-9). With the advantage of no cranium opening, anesthesia, or ionizing radiation, MRgFUS thalamotomy has become a research hotspot in the field of functional neurosurgery (10-12). However, the effect of focal ablation of the VIM on brain function and the mechanism of MRgFUS-induced tremor relief remain unclear. Resting-state functional magnetic resonance imaging (rsfMRI) data suggest that MRgFUS-induced tremor improvement in PD is relevant to the left occipital cortex involved in the visual area (11). Another diffusion tensor imaging (DTI) study revealed a U-shaped subnetwork sensitive to MRgFUS thalamotomy and a long-term dynamic loop (10). However, the effects of MRgFUS thalamotomy on structural MRI for gray matter volume (GMV) alteration in TDPD have never been explored.

Considering structural MRI, voxel-based morphometry (VBM) provides a better method of neuronal and glial cell density at a voxel precision level and uses routinely acquired T1-weighted imaging to study volume subparts and gray or white matter (WM) density (13-15). The regional alterations in GMV have been reported to be reliable for discriminating PD patients from healthy controls (HCs) versus different subtypes (16-19). Encouragingly, a series of studies have also demonstrated that tremor relief induced by VIM radiosurgery is associated with the visual area through gray matter (GM) analysis (20,21). These findings suggest the potential of GM alterations as a quantitative marker for PD to assess treatment response and hopefully provide data support for tremor suppression conveyed by MRgFUS thalamotomy.

The aim of the present study was to investigate possible GMV changes and their relationship with tremor symptoms from pre- to post-operation in TDPD. For this purpose, we performed a whole-brain investigation of GMV in cortical and subcortical structures and a correlation analysis between GMV changes and tremor improvement in TDPD patients with MRgFUS thalamotomy. This study is presented in accordance with the CONSORT (for pilot and feasibility trials) reporting checklist (available at https://qims.amegroups.com/article/view/10.21037/qims-22-1403/rc).

Methods

Participants

This study was conducted in accordance with the Declaration of Helsinki (as revised in 2013). The study was conducted with the approval of the Chinese PLA General Hospital ethics committee and was a part of a pilot clinical trial about the feasibility of MRgFUS thalamotomy in the treatment of TDPD (ClinicalTrials.gov identifier: NCT04570046). All patients provided written informed consent. Two neurologists with expertise in movement

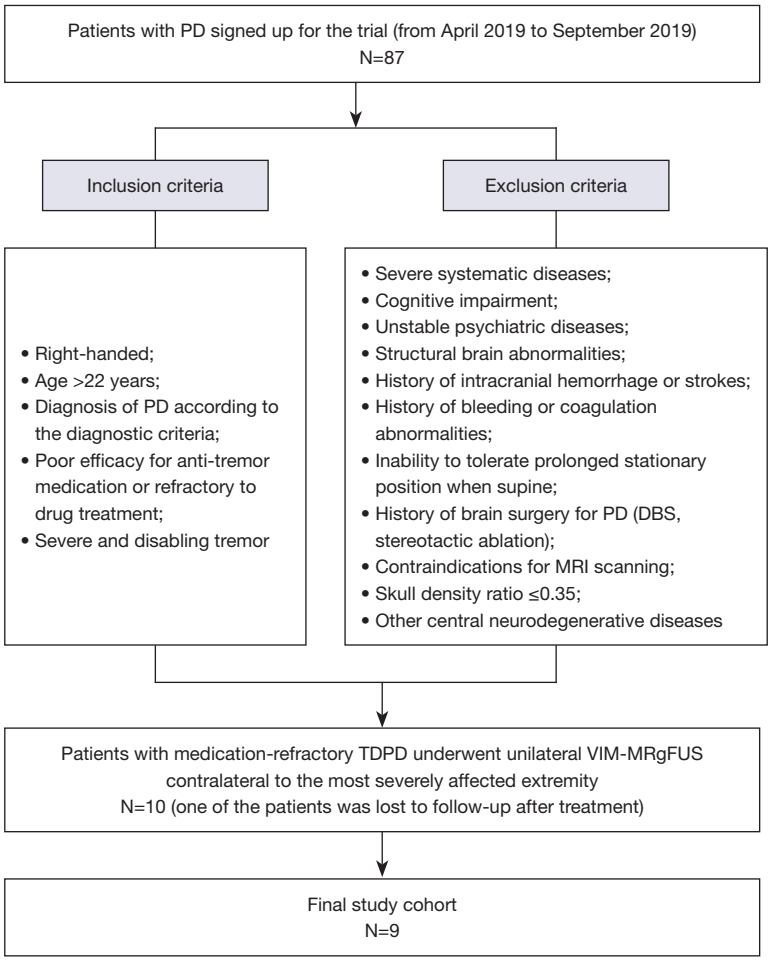

Figure 1 Flowchart of study patients with TDPD for MRgFUS thalamotomy. PD, Parkinson's disease; TDPD, tremor-dominant Parkinson's disease; DBS, deep brain stimulation; VIM, ventral intermedia nucleus; MRgFUS, magnetic resonance imaging-guided focused ultrasound; MRI, magnetic resonance imaging.

disorders diagnosed patients with PD. The criteria for the diagnosis of PD and dominance of the tremor were consistent with a previous report (22). The flowchart of study patients with TDPD for treatment is shown in *Figure 1*. We included 9 right-handed patients with TDPD who underwent MRgFUS treatment and target selection for the unilateral VIM nucleus contralateral to the most severely affected extremity. Nine age- and gender-matched right-handed HCs were also included for analysis.

MRgFUS thalamotomy procedure

All VIM-MRgFUS procedures were performed by the same neurosurgeon. The MRgFUS equipment was performed in a 3.0 T MRI suit (GE Discovery 750, GE Healthcare) using the 650-kHz ExAblate Neuro focused ultrasound system (InSightec, Haifa, Israel) with a hemispheric helmet and 1,024-element phased-array transducer. The ablative side was determined based on the severity of limb symptoms and the patient's personal willingness. The target was the VIM nucleus from triplanar T2-weighted images. The initial target ablation was performed using low-power sonication. Then, the energy for the final target ablation reached approximately 55–60 ℃ to ablative the target tissue, and the tremor in patients was well inhibited at this time.

Clinical evaluation and outcome measures after MRgFUS thalamotomy

For the HC group, clinical evaluations and MRI data were

collected at baseline. For patients, clinical evaluations were collected at baseline and at 1, 3 and 12 months of follow-up. MRI data were collected at baseline and 1 day, 7 days, 1 month, 3 months, and 12 months after surgery. Patients were assessed for tremors with the Clinical Rating Scale for Tremor (CRST) in the off-medication state. The CRST consists of three parts for evaluating tremor location/severity rating (Part A), specific motor tasks/functioning rating (Part B), and functional disabilities (Part C) (23). In addition, the treated hand tremor score was calculated by combining the CRST part A and CRST part B for the treated side. A higher score indicates more severe tremor. The total CRST scores for the dominant hand and the nondominant hand were 32 and 28, respectively. Additionally, tremor improvement from pre-operation to 1 year post-operation was calculated with the formula: (preoperative scores – postoperative scores)/preoperative scores ×100%.

MRI acquisition

All the participants underwent a standardized MRI protocol on a GE 3.0 T suite. High-resolution three-dimensional T1-weighted (T1-3D) with fast spoiled gradient recalled was used as the acquisition protocol, including the following parameters: repetition time (TR) =6.656 ms, echo time (TE) =2.928 ms, inversion time (TI) =800 ms, flip angle =7°, field of view (FOV) =256 mm, matrix =256×256, 192 contiguous sagittal 1-mm-thick slices.

MRI data preprocessing and analysis

Voxel-wise analysis

The MRI data were preprocessed using the longitudinal processing stream within the Computation Anatomy Toolbox (CAT 12) of the Statistical Parametric Mapping software (SPM12; Department of Neurology, London), performed with MATLAB 2013b (MathWorks, Boston, MA, USA). Prior to data processing, all images were inspected visually for motion or other artifacts and underwent manual reorientation. To keep the analysis consistent, the images of three patients with ablated right VIM nucleus were flipped along the x-axis. First, longitudinal images from all patients were rigidly aligned within patients, and the images were segmented into GM and WM and cerebrospinal fluid based (CSF) on tissue probability. Then, segmented tissue images were aligned to standard space to reduce bias between time points. After creating a study-specific GM template in standard space by using registration, GM segmentation from all patients was warped and normalized to this template. Finally, GM images were spatially smoothed using an 8-mm full-width-at-half-maximum (FWHM) Gaussian kernel to increase the signal-to-noise ratio.

Next, a whole brain voxel-wise paired *t*-test through SPM was used to identify significant changes in GMV from baseline to 1 year post-operation. We reported brain regions from the voxel level ($P<0.001$) and cluster level [$P<0.05$, family-wise error (FWE) correction]. The GMV with a significant difference was extracted from patients and HCs. We explored six time points to describe the dynamic changes in significant GMV. One-way repeated-measures analysis of variance (ANOVA) and *post-hoc* paired *t*-tests with Bonferroni corrections were used based on SPSS 26.0 statistical software (http://www.spss.com/). The extracted GMV from the patient groups and HC group was used to determine if the trend normalized for alterations induced by MRgFUS thalamotomy. The nonparametric Spearman rank correlation analysis was used to evaluate the longitudinal relationship between the changes in significant GMV induced by thalamotomy and changes in tremor scores over four time points. The significance threshold was set at 0.05, two-tailed.

ROI-wise analysis

The preprocessing procedure was consistent with previous studies (10). The Brainnetome atlas was used to identify 246 brain regions. A paired *t*-test was used to identify brain regions with significant ROI-wise GMV alterations from baseline to 12 months post-operation in patients with TDPD. The nonparametric Spearman rank test was used to study the correlation between the longitudinal changes in GMV and longitudinal changes in tremor scores.

To further evaluate GMV alterations, ROIs were also defined as brain regions in the basal ganglia and related nuclei and cerebellum subregions. The integrated registration and segmentation tool based on the FMRIB Software Library (http://fsl.fmrib.ox.ac.uk/fsl/fslwiki/) was used to estimate the absolute volumes of the basal ganglia and related nuclei (14). This procedure included linearly registering the original T1-weighted image into the MNI152 1-mm template, secondary registration and automatic segmentation of the basal ganglia and related nuclei and boundary correction to remove extraneous voxels on the surface of the mesh segmentation. Finally, we

Table 1 Demographic and clinical characteristics of included participants with TDPD and HC

Variables	TDPD	HC	t	P
Age (years)	64.67±6.12	60.11±6.74	1.501	0.153
Male/female	8/1	8/1	–	–
Disease duration (years)	8.22±7.19	–	–	–
LEDD (mg/day)	618.22±188.20	–	–	–
Lesion side (L/R)	6/3	–	–	–
SDR	0.53±0.14	–	–	–
MMSE	28.00±1.50	–	–	–
Peak temperature (℃)	57.89±1.53	–	–	–
Tremor improvement (%)	74.82±15.33	–	–	–

Data are presented as the mean ± standard deviation or number. Tremor improvement represents improvement in tremor of treated hand. TDPD, tremor-dominant Parkinson's disease; HC, healthy control; LEDD, levodopa-equivalent daily dose; L, left; R, right; SDR, skull density ratio; MMSE, Mini-mental State Examination.

acquired ROI volumes in the bilateral amygdala, accumbens nucleus, thalamus, caudate, putamen, hippocampus, and pallidum.

Next, the SUIT toolbox (http://www.diedrichsenlab.org/imaging/suit_function.htm), a tool based on SPM12, calculated cerebellar volumes (16). The cerebellum was isolated on T1-3D images of TDPD patients. Then, the isolated cerebellum was normalized to the SUIT atlas by using the affine transformation matrix and nonlinear flow field. After normalization, the cerebellum was resliced according to the SUIT atlas to obtain the cerebellar subregion volumes. Next, the resulting SUIT atlas was realigned back to the native participant space. Lobuli-ROI analysis with atlas was used to calculate the volume of the cerebellar lobules, which were computed as the sum of the hemispheres and vermis after being normalized for total intracranial volume (TIV). Finally, the volume of all the lobules was summed together to obtain the whole cerebellum volume, whereas the sum of lobules I–V and VI–X was used to calculate the anterior and posterior cerebellar volumes, respectively. The dynamic GMV alterations of ROIs over six time points in patients were calculated in the same way as the voxel-wise level.

Results

The group of 9 TDPD participants who underwent MRgFUS thalamotomy was characterized by an age of 64.67±6.12 years (8 males) and a disease duration of 8.22±7.19 years. Demographic and clinical characteristics of the included TDPD patients and HCs are shown in *Table 1*. Four patients experienced mild dizziness after treatment, which was relieved within 24 hours. No other side effects were found 1 year after MRgFUS thalamotomy. Tremors were significantly relieved after MRgFUS thalamotomy in all patients (P<0.05). The treated hand tremor scores improved by a mean of 74.82% in patients at 12 months post-operation. The hand tremor score on the treated side decreased from 16.78±3.73 points preoperatively to 4.00±2.18 points at 12 months after sonication (t=8.750; P<0.001), and the CRST total score decreased from 45.89±8.94 to 17.89±11.92 (t=8.247; P<0.001) (*Table 2*, *Figure 2A*,*2B*).

Voxel-wise level of GMV in patients with TDPD after MRgFUS thalamotomy

The analysis at the voxel-wise level revealed a significant decrease in GMV in the left middle occipital gyrus (MOG) (*Figure 2C*; *Table 3*) and an increase in GMV in the left precentral gyrus (PreCG) (*Figure 2D*; *Table 3*) from baseline to the 12-month follow-up.

Longitudinal analysis showed GMV of the left MOG was in the decreasing shift versus the left PreCG was toward normality during follow-up after MRgFUS thalamotomy. *Post-hoc* tests revealed significant differences in the left MOG (df=5, F=3.49, P=0.01) (*Figure 2E*) and left PreCG (df=5, F=2.397, P=0.054) (*Figure 2F*) between pre- and

Table 2 The clinical rating subscale for tremor in all MRgFUS participants

Clinical scores	Pre-operation	12-month post-operation	*t* value	P value
Hand tremor score	16.78±3.73	4.00±2.18	8.750	<0.001
CRST total	45.89±8.94	17.89±11.92	8.247	<0.001
CRST A	20.78±3.73	7.33±4.15	9.847	<0.001
CRST B	11.11±5.01	3.44±3.64	7.889	<0.001
CRST C	14.00±3.50	7.11±8.30	2.413	<0.05

Data are presented as the mean ± standard deviation. P value from paired *t*-tests compared with corresponding scores at the pre-operation. MRgFUS, magnetic resonance imaging-guided focused ultrasound; CRST, the Clinical Rating Scale for Tremor.

post-operation. Furthermore, compared to HCs, GMV in the left MOG was decreased from baseline to the 12-month follow-up (*Figure 3A*). Additionally, GMV in the left PreCG in patients was elevated after thalamotomy compared with that in HCs (*Figure 3A*).

Importantly, the decreasing trend of GMV in the left MOG was positively correlated with changes in tremor scores for four time points (CRST total score: rho =0.384, P=0.021; CRST A score: rho =0.346, P=0.039; CRST C score: rho =0.439, P=0.007; df=34) (*Figure 3B*). Different types of tremor scores further showed significant negative correlations between the increasing trend of GMV in the left PreCG and rest or postural tremor improvement (rest tremor: rho =−0.493, P=0.002; postural tremor: rho =−0.411, P=0.013; df=34) (*Figure 3B,3C*).

ROI-wise level of GMV in patients with TDPD after MRgFUS thalamotomy

A paired-sample Student's *t*-test identified 24 brain regions associated with significant differences at 12 months after thalamotomy (P<0.05) (Table S1). It was obvious that the tremor-related GMV regions were mainly concentrated within the parietal lobe and the occipital lobe, which included the rostroventral area of the inferior parietal lobule (A39rv), the dorsomedial parietooccipital sulcus of the precuneus (dmPOS), the rostral cuneus gyrus (rCunG) and the ventromedial parietooccipital sulcus (vmPOS) of the medio ventral occipital cortex on the right side (*Figure 3D-3G*). In addition, A39rv was correlated with CRST C (r=0.488, P=0.04). Other tremor-related GMV regions were significantly correlated with CRST B (dmPOS: r=−0.506, P=0.032; rCunG: r=−0.624, P=0.006; vmPOS: r=−0.624, P=0.006).

There were also significant differences with Bonferroni correction in GMV for the left thalamus (df=5, F=11.1, P<0.01; *Figure 4*) and cerebellum subregions in right V, vermis VI, vermis crus II and vermis VIIb (df=5, 2.3<F<4.2, P<0.05) (*Figure 5*) after MRgFUS thalamotomy. There was no significant difference in the other cerebellum regions (Figure S1).

Discussion

This study quantitatively evaluated GMV alterations in patients with TDPD who underwent MRgFUS thalamotomy. We found significant alterations in voxel-wise GMV in the left MOG and the left PreCG after treatment in TDPD patients, which correlated with tremor improvement. Furthermore, ROI-wise GMV related to MRgFUS thalamotomy was also associated with long-term structural alterations.

The purpose of this study was to explore the impacts on GMV induced by MRgFUS thalamotomy in patients with TDPD and to learn whether GMV alterations could reveal the neural remodeling of tremor suppression after thalamotomy. Our findings suggested that MRgFUS thalamotomy had an effect on the different GMVs with a dynamic change process. Specifically, significant clusters mediated by MRgFUS thalamotomy were detected in the left occipital gyrus and the left PreCG. The former cluster included the left MOG and the left inferior occipital gyrus involved in the visual area. The latter was the left PreCG involved in the primary motor area (M1). Additionally, it is unclear whether a decrease in the left MOG is actually due to the procedure or part of the neurodegenerative process or MRgFUS intervention. Hanganu *et al.* suggested that PD patients at the early stage of mild cognitive impairment were correlated with a faster process of GM thinning in different cortical regions at the 20-month follow-up, including the

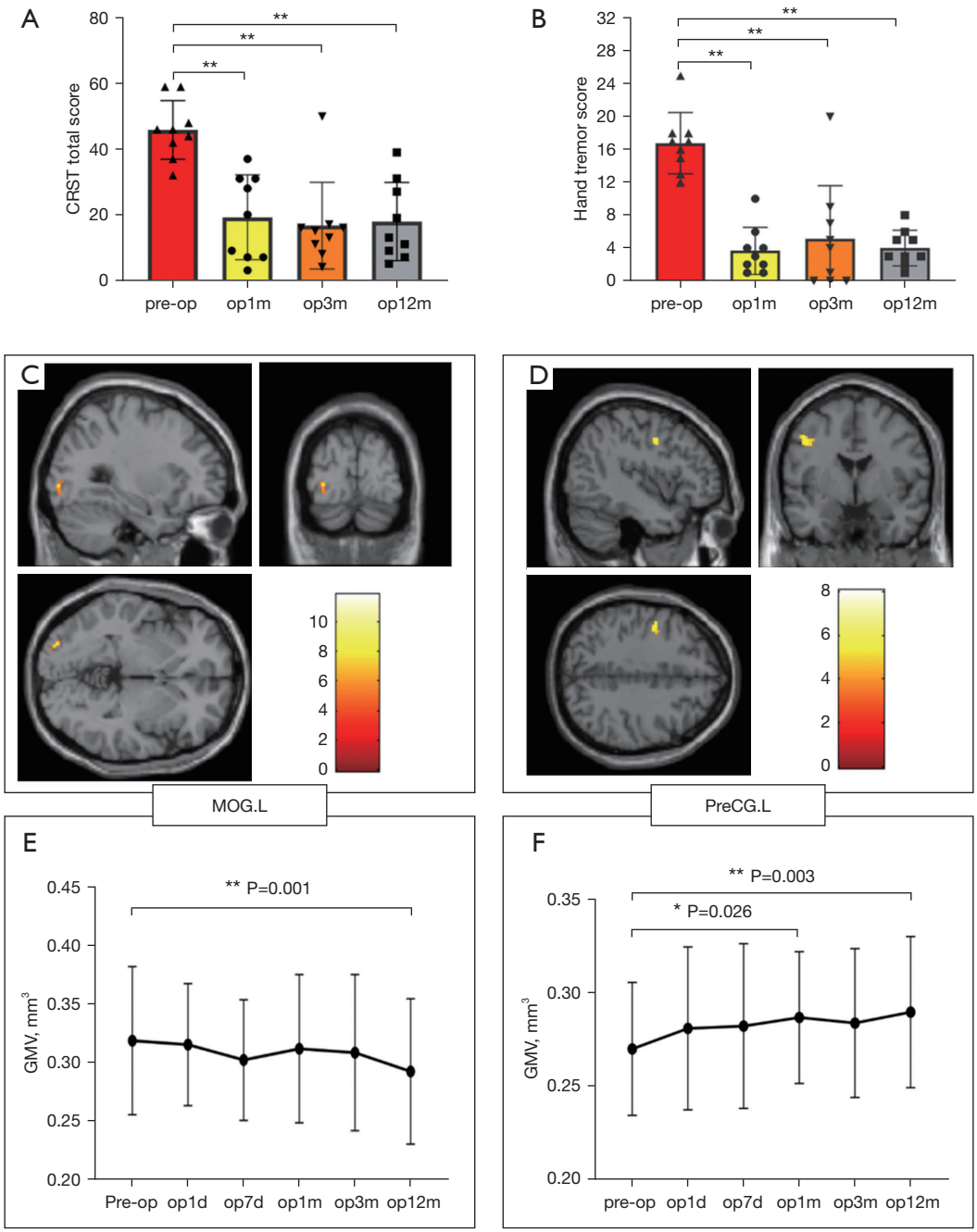

Figure 2 Tremor improvement and alteration in voxel-wise level of GMV for patients with TDPD after MRgFUS thalamotomy. (A,B) Bar graphs of CRST total and hand tremor scores at different time points. (C) GMV was significantly decreased in the left MOG from pre-operation to 12 months post-operation (voxel-level P<0.001, cluster-level P_{FWE} <0.05). (D) GMV was significantly increased in the left PreCG from pre-operation to 12 months post-operation (voxel-level P<0.001, cluster-level P_{FWE} <0.05). (E,F) Dynamic alterations in GMV in the left MOG and left PreCG. The color bar shows the T score. *, P<0.05; **, P<0.01. Bonferroni correction for P value (α=0.01). CRST, clinical rating scale for tremor; FWE, family-wise error; GMV, gray matter volume; MRgFUS, magnetic resonance imaging-guided focused ultrasound; MOG.L, left middle occipital gyrus; PreCG.L, left precentral gyrus; TDPD, tremor-dominant Parkinson's disease; pre-op, pre-operation; op1d, 1 day post-operation; op7d, 7 days post-operation; op1m, 1 month post-operation; op3m, 3 months post-operation; op12m, 12 months post-operation.

Table 3 Voxel-wise analysis for altered GMV in TDPD patients from baseline to 12 months after MRgFUS thalamotomy

MNI coordinate region	Side	Cluster size (voxels)	Peak MNI coordinate (mm)			Peak-level *t* value	Voxel-level P	Cluster-level P_{FWE}
			x	y	z			
Cluster 1: pre-operation >12-month post-operation								
MOG	L	46	–27	–90	–1.5	11.81	<0.001	<0.05*
IOG	L	104	–	–	–	–	–	–
Cluster 2: 12-month post-operation > pre-operation								
PreCG	L	142	–34.5	0	43.5	7.99	<0.001	<0.05*

*, voxel-level P<0.001, cluster-level P_{FWE}<0.05. GMV, gray matter volume; TDPD, tremor-dominant Parkinson's disease; MRgFUS, magnetic resonance imaging-guided focused ultrasound; MNI, Montreal Neurological Institute; FWE, family-wise error; MOG, middle occipital gyrus; IOG, inferior occipital gyrus; PreCG, precentral gyrus; L, left.

temporal, occipital, parietal and supplementary motor areas (24). A link between occipital GMV reduction and visual hallucinations in PD has also been reported (25). However, evidence for changes in GM patterns within a year is still lacking. Therefore, we might speculate that alterations in GMV in the visual area and M1 might be a distant effect of MRgFUS thalamotomy.

However, tremor generation and further tremor control for MRgFUS thalamotomy from the viewpoint of brain function in the visual areas are not clear. Previous studies speculated that the input from the visual to the contralateral motor network could be calibrated through a series of cortical-cortical connections by the corpus callosum, by the basal ganglia (caudate and claustrum) or by the cerebellum (26,27). A study employed 2 distinct neuroimaging modalities to specifically investigate function-structure interrelationships that are related to parkinsonism, showing a significant correlation between a structural component (GMV) and a rsfMRI component [fractional amplitude of low-frequency fluctuation (fALFF)] (28). Therefore, research on rsfMRI cannot be ignored. Xiong *et al.* reported that the left occipital cortex in the visual area has demonstrated abnormalities in local neuronal activity as measured by fALFF in TDPD (11). According to the Brodmann area (BA), the alteration in fALFF involved in this study is located in BA17, while our altered GM regions belong to BA18. The authors further concluded that the left occipital cortex is involved in specific visuomotor networks and might exhibit a distant effect of MRgFUS thalamotomy on tremor control in PD. Tuleasca *et al.* also provided data support that thalamotomy could cause alterations in structural and functional networks in visual regions in essential tremor (ET) patients (29). They used rsfMRI to conduct whole-brain analysis through data-driven multivariate analysis, concluding that VIM radiosurgery probably tended to normalize interconnectivity in visual areas for all patients with ET, but patients with more functional integration in visual regions at pre-operation could have a better outcome (27). Based on VBM analysis, they also reported that pretherapeutic GM density in the right extrastriate cortex BA18 could predict tremor improvement on the right treated hand at 12 months post-operation (20). Interestingly, another study reported that the left temporal pole and occipital BA19 were statistically significant, and this decrease in GMV correlated with higher tremor scores on treated hand improvement (21). The two studies showed that the directionality of the significant cluster was different, and our results were consistent with the latter. These findings suggest that the importance of alterations in the visual areas due to different treatments of the VIM nucleus for tremor relief cannot be ignored and support our study in which the GMV of the visual areas was associated with tremor improvement in TDPD.

The PreCG could be of equal importance in tremor generation and further tremor control. Given prior experience in ET, one rsfMRI study showed that an increase in functional activity by fALFF in the bilateral PreCG and left supplemental motor cortex for these brain networks was negatively correlated with tremor scores after MRgFUS thalamotomy (30). Another study also suggested that tremor relief induced by ablating the VIM nucleus was correlated with sensorimotor and attention networks, and preoperative functional connection strengths could predict tremor response to guide clinical practice (31). A significant increase in GMV in the left PreCG was detected

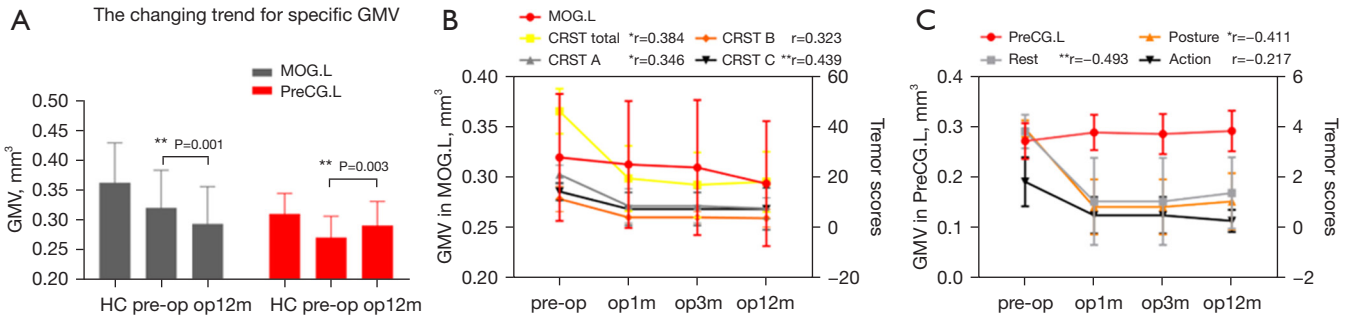

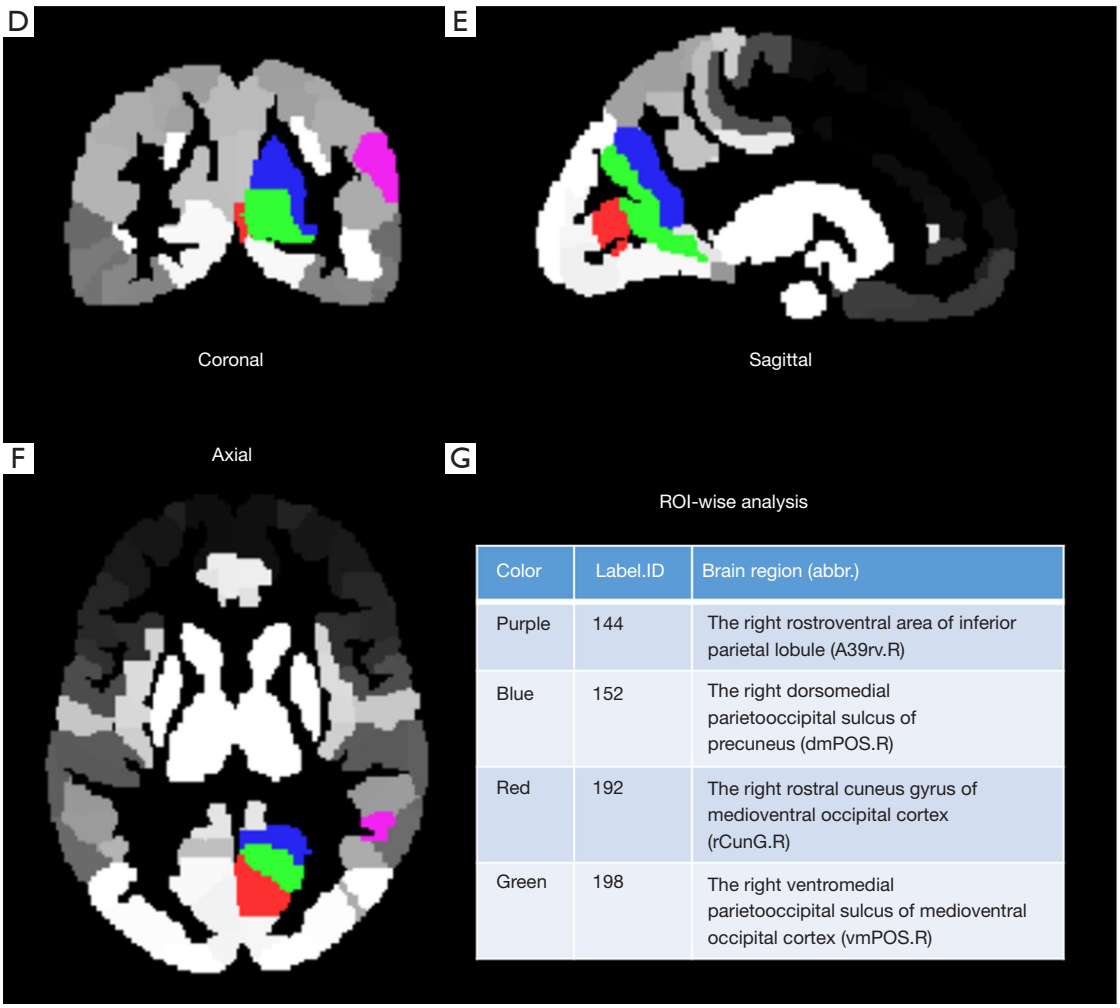

Color	Label.ID	Brain region (abbr.)
Purple	144	The right rostroventral area of inferior parietal lobule (A39rv.R)
Blue	152	The right dorsomedial parietooccipital sulcus of precuneus (dmPOS.R)
Red	192	The right rostral cuneus gyrus of medioventral occipital cortex (rCunG.R)
Green	198	The right ventromedial parietooccipital sulcus of medioventral occipital cortex (vmPOS.R)

Figure 3 The relationship between the changing trend of GMV and tremor scores. Voxel-wise analysis: (A) the changing trend for specific GMV mediated by MRgFUS between HCs and patients at pre-operation and 12 months post-operation. (B) The falling trend of GMV in the left MOG and related tremor scores had a significant positive relationship. Tremor scores include CRST total score, CRST A score, CRST B score, and CRST C score. (C) A significant negative correlation between the increasing trend of GMV in the left PreCG and related tremor scores. Tremor scores include resting tremor score, postural tremor score, and action tremor score. ROI-wise analysis: coronal (D), sagittal (E), and axial (F) diagrams of the correlation between the ROI-GMV and tremor scores at pre-operation and 12 months post-operation. (G) ROI-GMV in the brain region information. The Brainnetome atlas was used to describe ROI-GMV. *, P<0.05; **, P<0.01. GMV, gray matter volume; MRgFUS, magnetic resonance imaging-guided focused ultrasound; HC, healthy control, MOG.L, left middle occipital gyrus; CRST, clinical rating scale for tremor; PreCG.L, left precentral gyrus; ROI, region of interest.

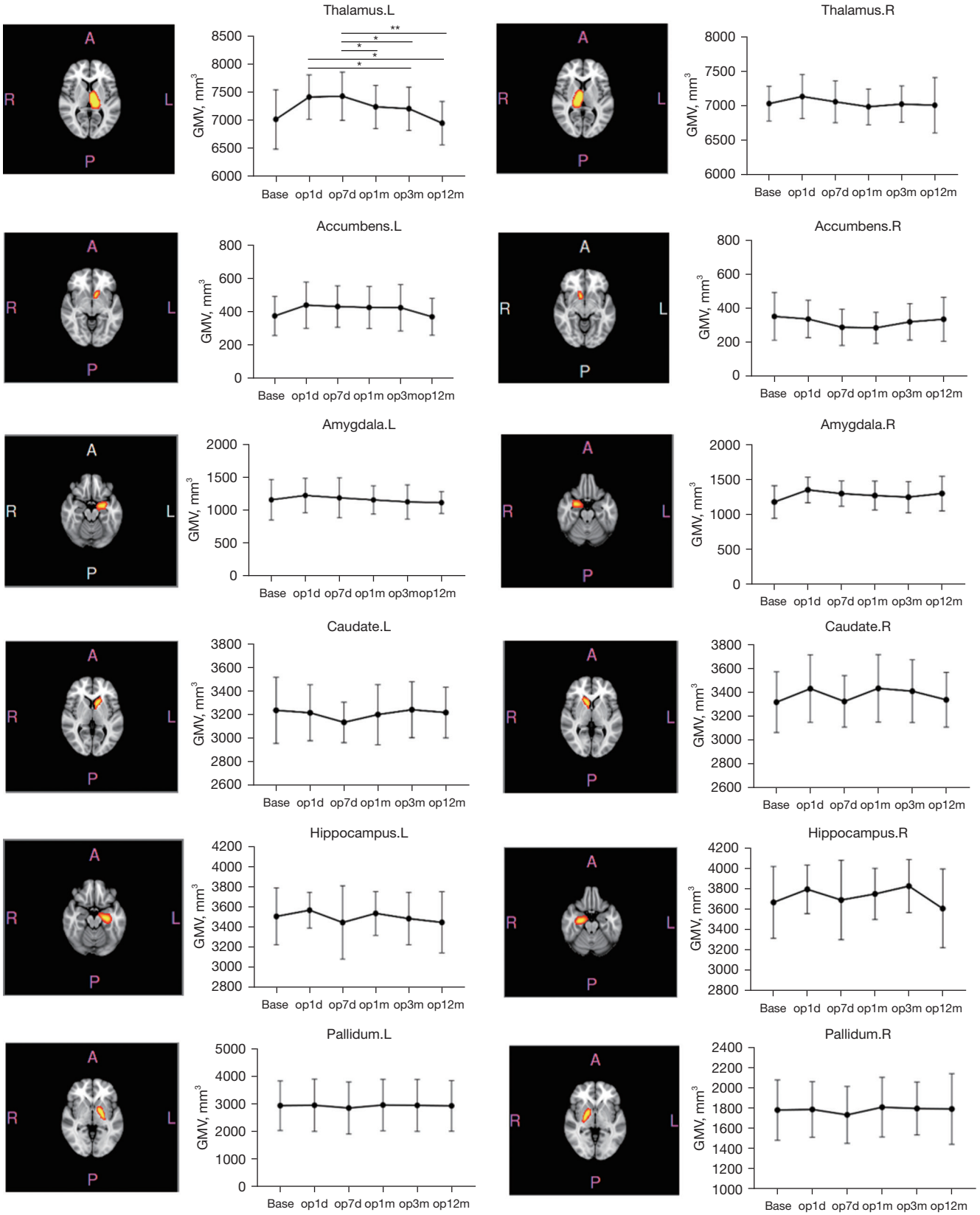

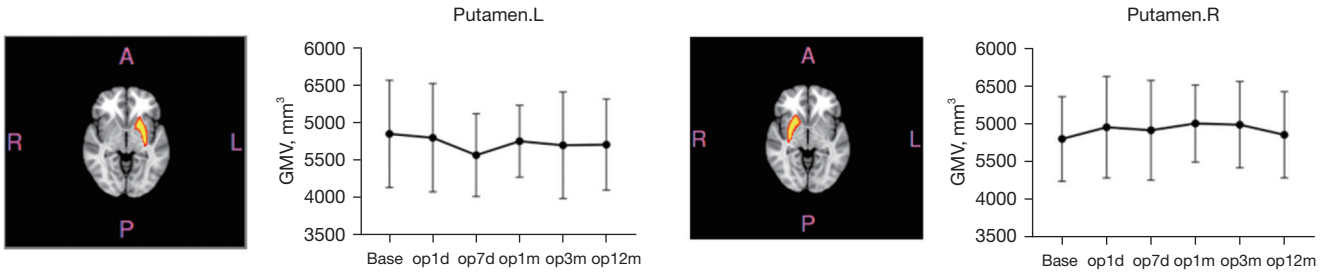

Figure 4 The changing trends in GMV in the basal ganglia and related nuclei after MRgFUS thalamotomy. *, P<0.05; **, P<0.01 with Bonferroni correction. GMV, gray matter volume; MRgFUS, magnetic resonance imaging-guided focused ultrasound; op1d, 1 day post-operation; op7d, 7 days post-operation; op1m, 1 month post-operation; op3m, 3 months post-operation; op12m, 12 months post-operation; A, anterior; P, posterior; L, left; R, right.

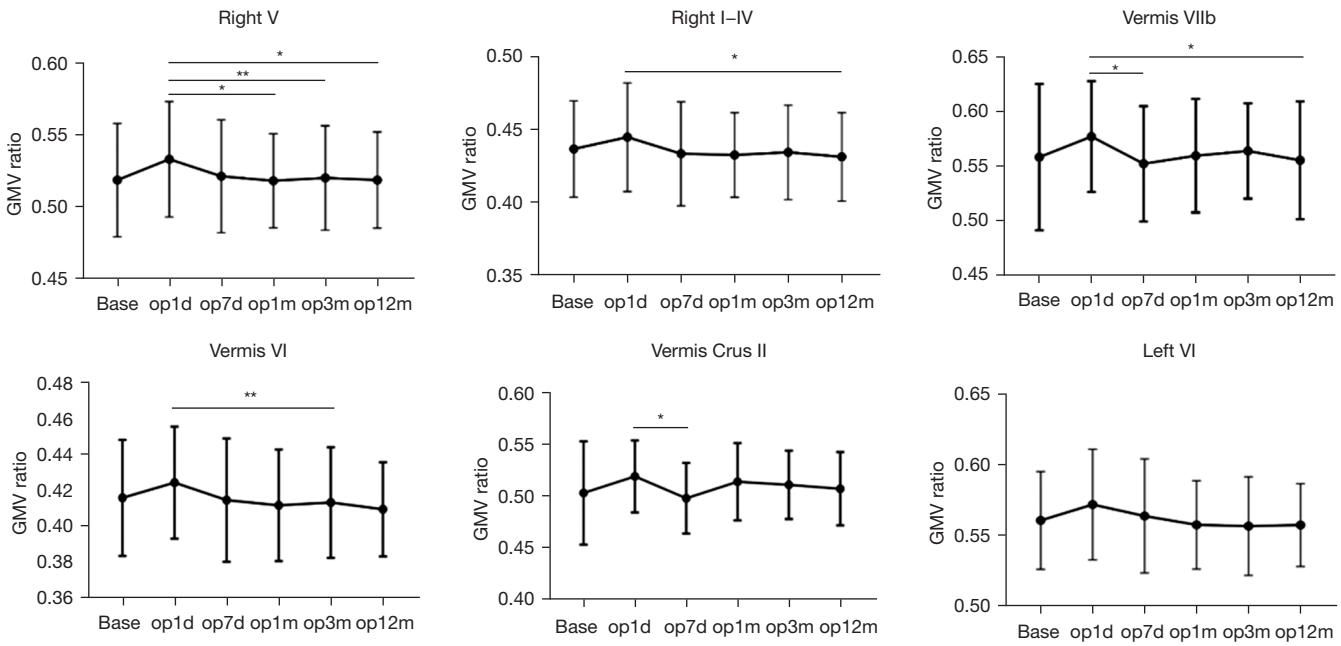

Figure 5 The changing trends in GMV in cerebellar subregions after MRgFUS thalamotomy. *, P<0.05; **, P<0.01 with Bonferroni correction. GMV, gray matter volume; MRgFUS, magnetic resonance imaging-guided focused ultrasound; op1d, 1 day post-operation; op7d, 7 days post-operation; op1m, 1 month post-operation; op3m, 3 months post-operation; op12m, 12 months post-operation.

in our study, which was also related to tremor scores. It is reasonable to assume that this cluster-level significant difference was involved in tremor control through the CTC circuit. An animal experiment revealed that a somatotopically organized closed loop consisted of input from the cerebellar lobules and output from the granular layer of the same cerebellar lobules in the arm area of M1 (32). The anterior cerebellum lobule IV–V, dentate nucleus, and M1 had more metabolic activity in a positron emission tomography (PET) study, which correlated with unified Parkinson's disease rating scale (UPDRS) tremor subscale ratings in TDPD (33). These findings support the role of the PreCG in tremor control in PD.

The longitudinal study for ROI-wise analyses showed that GMV related to MRgFUS thalamotomy was at long-term structural alterations. We found that four related tremor GMVs were mainly located in the parietal lobe and the occipital lobe. Our purpose was not to reveal the detailed internal mechanism; rather, we are interested

in finding that GMV was altered at the ROI level at 12 months after surgery. Additionally, there were also significant differences in GMV for the left thalamus and cerebellum subregions in right V, vermis VI, vermis crus II and vermis VIIb, suggesting that these GMV regions were dynamically changed by ablating the VIM nucleus. Interestingly, a previous study showed that the enlarged thalamic volume (mainly in the ventral lateral) was correlated with tremor severity in TDPD (34). The average clinical tremor improvement in TDPD patients was more than 60%; however, we did not find a significant difference in the GMV of the left thalamus at 12 months post-operation compared to pre-operation. The voxel-level analysis for GM also found no related thalamic changes in a study for VIM radiosurgery at the 12-month follow-up, although tremor scores of these patients on the treated hand had at least 50% improvement (21). Further studies are needed to address these issues. In addition, there was also no significant difference in the GMV of cerebellar subregions at 12 months post-operation. Tremor improvement induced by MRgFUS in TDPD patients is accompanied by the influence of ROI-wise GMV from baseline to 12 months post-operation. Could these changes be protective mechanisms for patients accompanying symptom improvement? Caution should be exercised because different methods may yield inconsistent results. More research is needed in the future.

The main limitation of this study was the small sample size. We included longitudinal data to enhance study sensitivity, but larger sample studies are still needed in the future. Although GMV changes were associated with clinical symptoms at 1 year post-operation, longer longitudinal studies are still necessary to detect the evolution beyond 1 year. Additionally, we used a highly stringent statistical threshold of 0.05 for FWE correction, so our study might be underpowered to detect some minor alterations in the GMV of the brain in PD patients after MRgFUS thalamotomy; therefore, other correction methods are also worth exploring.

Conclusions

This is the first study to evaluate long-term GMV alterations in brain architecture for MRgFUS thalamotomy. It not only identifies GMV alterations in the left MOG and left PreCG sensitive to MRgFUS thalamotomy but also suggests a long-term dynamic process involved in GMV for MRgFUS thalamotomy. Therefore, it might be helpful to better understand the distant neural remodeling for MRgFUS thalamotomy and GMV alterations in tremor control in TDPD.

Acknowledgments

Funding: This work was supported by the National Natural Science Foundation of China (Nos. 82151309 and 81825012, to Xin Lou).

Footnote

Reporting Checklist: The authors have completed the CONSORT (for pilot and feasibility trials) reporting checklist. Available at https://qims.amegroups.com/article/view/10.21037/qims-22-1403/rc

Conflicts of Interest: All authors have completed the ICMJE uniform disclosure form (available at https://qims.amegroups.com/article/view/10.21037/qims-22-1403/coif). The authors have no conflicts of interest to declare.

Ethical Statement: The authors are accountable for all aspects of the work in ensuring that questions related to the accuracy or integrity of any part of the work are appropriately investigated and resolved. This study was conducted in accordance with the Declaration of Helsinki (as revised in 2013). The study was conducted with the approval of the Chinese PLA General Hospital ethics committee and was a part of a pilot clinical trial about the feasibility of MRgFUS thalamotomy in the treatment of TDPD (ClinicalTrials.gov identifier: NCT04570046). All patients provided written informed consent.

References

1. Thenganatt MA, Jankovic J. Parkinson disease subtypes. JAMA Neurol 2014;71:499-504.

2. Helmich RC, Hallett M, Deuschl G, Toni I, Bloem BR. Cerebral causes and consequences of parkinsonian resting tremor: a tale of two circuits? Brain 2012;135:3206-26.
3. Helmich RC. The cerebral basis of Parkinsonian tremor: A network perspective. Mov Disord 2018;33:219-31.
4. Riou A, Houvenaghel JF, Dondaine T, Drapier S, Sauleau P, Drapier D, Duprez J, Guillery M, Le Jeune F, Verin M, Robert G. Functional Role of the Cerebellum in Parkinson Disease: A PET Study. Neurology 2021;96:e2874-84.
5. Bond AE, Shah BB, Huss DS, Dallapiazza RF, Warren A, Harrison MB, Sperling SA, Wang XQ, Gwinn R, Witt J, Ro S, Elias WJ. Safety and Efficacy of Focused Ultrasound Thalamotomy for Patients With Medication-Refractory, Tremor-Dominant Parkinson Disease: A Randomized Clinical Trial. JAMA Neurol 2017;74:1412-8.
6. Meng Y, Pople CB, Kalia SK, Kalia LV, Davidson B, Bigioni L, Li DZ, Suppiah S, Mithani K, Scantlebury N, Schwartz ML, Hamani C, Lipsman N. Cost-effectiveness analysis of MR-guided focused ultrasound thalamotomy for tremor-dominant Parkinson's disease. J Neurosurg 2020. [Epub ahead of print]. doi: 10.3171/2020.5.JNS20692.
7. Wang X, Xiong Y, Lin J, Lou X. Target Selection for Magnetic Resonance-Guided Focused Ultrasound in the Treatment of Parkinson's Disease. J Magn Reson Imaging 2022;56:35-44.
8. Zaaroor M, Sinai A, Goldsher D, Eran A, Nassar M, Schlesinger I. Magnetic resonance-guided focused ultrasound thalamotomy for tremor: a report of 30 Parkinson's disease and essential tremor cases. J Neurosurg 2018;128:202-10.
9. Yamamoto K, Ito H, Fukutake S, Odo T, Kamei T, Yamaguchi T, Taira T. Focused Ultrasound Thalamotomy for Tremor-dominant Parkinson's Disease: A Prospective 1-year Follow-up Study. Neurol Med Chir (Tokyo) 2021;61:414-21.
10. Lin J, Kang X, Xiong Y, Zhang D, Zong R, Yu X, Pan L, Lou X. Convergent structural network and gene signatures for MRgFUS thalamotomy in patients with Parkinson's disease. Neuroimage 2021;243:118550.
11. Xiong Y, Han D, He J, Zong R, Bian X, Duan C, Zhang D, Zhou X, Pan L, Lou X. Correlation of visual area with tremor improvement after MRgFUS thalamotomy in Parkinson's disease. J Neurosurg 2021;136:681-8.
12. Xiong Y, Lin J, Pan L, Zong R, Bian X, Duan C, Zhang D, Lou X. Pretherapeutic functional connectivity of tractography-based targeting of the ventral intermediate nucleus for predicting tremor response in patients with Parkinson's disease after thalamotomy with MRI-guided focused ultrasound. J Neurosurg 2022. [Epub ahead of print]. doi: 10.3171/2022.1.JNS212449.
13. Albrecht F, Pereira JB, Mijalkov M, Freidle M, Johansson H, Ekman U, Westman E, Franzén E. Effects of a Highly Challenging Balance Training Program on Motor Function and Brain Structure in Parkinson's Disease. J Parkinsons Dis 2021;11:2057-71.
14. Pietracupa S, Bologna M, Bharti K, Pasqua G, Tommasin S, Elifani F, Paparella G, Petsas N, Grillea G, Berardelli A, Pantano P. White matter rather than gray matter damage characterizes essential tremor. Eur Radiol 2019;29:6634-42.
15. Gellersen HM, Guo CC, O'Callaghan C, Tan RH, Sami S, Hornberger M. Cerebellar atrophy in neurodegeneration-a meta-analysis. J Neurol Neurosurg Psychiatry 2017;88:780-8.
16. Xu X, Han Q, Lin J, Wang L, Wu F, Shang H. Grey matter abnormalities in Parkinson's disease: a voxel-wise meta-analysis. Eur J Neurol 2020;27:653-9.
17. Sarasso E, Agosta F, Piramide N, Filippi M. Progression of grey and white matter brain damage in Parkinson's disease: a critical review of structural MRI literature. J Neurol 2021;268:3144-79.
18. Chen J, Jiang X, Wu J, Wu H, Zhou C, Guo T, Bai X, Liu X, Wen J, Cao Z, Gu L, Yang W, Pu J, Guan X, Xu X, Zhang B, Zhang M. Gray and white matter alterations in different predominant side and type of motor symptom in Parkinson's disease. CNS Neurosci Ther 2022;28:1372-9.
19. Kuhn T, Becerra S, Duncan J, Spivak N, Dang BH, Habelhah B, Mahdavi KD, Mamoun M, Whitney M, Pereles FS, Bystritsky A, Jordan SE. Translating state-of-the-art brain magnetic resonance imaging (MRI) techniques into clinical practice: multimodal MRI differentiates dementia subtypes in a traditional clinical setting. Quant Imaging Med Surg 2021;11:4056-73.
20. Tuleasca C, Witjas T, Van de Ville D, Najdenovska E, Verger A, Girard N, Champoudry J, Thiran JP, Cuadra MB, Levivier M, Guedj E, Régis J. Right Brodmann area 18 predicts tremor arrest after Vim radiosurgery: a voxel-based morphometry study. Acta Neurochir (Wien) 2018;160:603-9.
21. Tuleasca C, Witjas T, Najdenovska E, Verger A, Girard N, Champoudry J, Thiran JP, Van de Ville D, Cuadra MB, Levivier M, Guedj E, Régis J. Assessing the clinical outcome of Vim radiosurgery with voxel-based morphometry: visual areas are linked with tremor arrest! Acta Neurochir (Wien) 2017;159:2139-44.
22. Jankovic J, McDermott M, Carter J, Gauthier S, Goetz C, Golbe L, Huber S, Koller W, Olanow C, Shoulson

I. Variable expression of Parkinson's disease: a base-line analysis of the DATATOP cohort. The Parkinson Study Group. Neurology 1990;40:1529-34.
23. Stacy MA, Elble RJ, Ondo WG, Wu SC, Hulihan J; . Assessment of interrater and intrarater reliability of the Fahn-Tolosa-Marin Tremor Rating Scale in essential tremor. Mov Disord 2007;22:833-8.
24. Hanganu A, Bedetti C, Degroot C, Mejia-Constain B, Lafontaine AL, Soland V, Chouinard S, Bruneau MA, Mellah S, Belleville S, Monchi O. Mild cognitive impairment is linked with faster rate of cortical thinning in patients with Parkinson's disease longitudinally. Brain 2014;137:1120-9.
25. Ramírez-Ruiz B, Martí MJ, Tolosa E, Giménez M, Bargalló N, Valldeoriola F, Junqué C. Cerebral atrophy in Parkinson's disease patients with visual hallucinations. Eur J Neurol 2007;14:750-6.
26. Glickstein M. How are visual areas of the brain connected to motor areas for the sensory guidance of movement? Trends Neurosci 2000;23:613-7.
27. Tuleasca C, Najdenovska E, Régis J, Witjas T, Girard N, Champoudry J, Faouzi M, Thiran JP, Cuadra MB, Levivier M, Van De Ville D. Clinical response to Vim's thalamic stereotactic radiosurgery for essential tremor is associated with distinctive functional connectivity patterns. Acta Neurochir (Wien) 2018;160:611-24.
28. Wolf RC, Rashidi M, Fritze S, Kubera KM, Northoff G, Sambataro F, Calhoun VD, Geiger LS, Tost H, Hirjak D. A Neural Signature of Parkinsonism in Patients With Schizophrenia Spectrum Disorders: A Multimodal MRI Study Using Parallel ICA. Schizophr Bull 2020;46:999-1008.
29. Tuleasca C, Régis J, Najdenovska E, Witjas T, Girard N, Thiran JP, Bach Cuadra M, Levivier M, Van De Ville D. Visually-sensitive networks in essential tremor: evidence from structural and functional imaging. Brain 2018;141:e47.
30. Xiong Y, Lin J, Bian X, Lu H, Zhou J, Zhang D, Pan L, Lou X. Treatment-Specific Network Modulation of MRI-Guided Focused Ultrasound Thalamotomy in Essential Tremor : Modulation of ET-Related Network by MRgFUS Thalamotomy. Neurotherapeutics 2022;19:1920-31.
31. Lu H, Lin J, Xiong Y, Deng L, Wang X, Zhang D, Bian X, Zhou J, Pan L, Lou X. Assessing the impact of MR-guided focused ultrasound thalamotomy on brain activity and connectivity in patients with essential tremor. Neurosurg Focus 2022;53:E5.
32. Kelly RM, Strick PL. Cerebellar loops with motor cortex and prefrontal cortex of a nonhuman primate. J Neurosci 2003;23:8432-44.
33. Mure H, Hirano S, Tang CC, Isaias IU, Antonini A, Ma Y, Dhawan V, Eidelberg D. Parkinson's disease tremor-related metabolic network: characterization, progression, and treatment effects. Neuroimage 2011;54:1244-53.
34. Jia X, Liang P, Li Y, Shi L, Wang D, Li K. Longitudinal Study of Gray Matter Changes in Parkinson Disease. AJNR Am J Neuroradiol 2015;36:2219-26.

Cite this article as: Wang X, Wang S, Lin J, Zhang D, Lu H, Xiong Y, Deng L, Zhang D, Bian X, Zhou J, Pan L, Lou X. Gray matter alterations in tremor-dominant Parkinson's disease after MRgFUS thalamotomy are correlated with tremor improvement: a pilot study. Quant Imaging Med Surg 2023;13(7):4415-4428. doi: 10.21037/qims-22-1403

Supplementary

Table S1 ROI-wise analysis for altered GMV in PD patients at 12 months after MRgFUS thalamotomy compared with baseline

Label. ID	Gyrus	Brain region	Side	Anatomical and modified cyto-architectonic descriptions	MNI (x, y, z)	t value	P value*
30	Frontal lobe	Inferior frontal gyrus (IFG)	R	A44d: dorsal area 44	45, 16, 25	3.289	0.011
54		Precentral gyrus (PrG)	R	A4hf: area 4 (head and face region)	55, −2, 33	3.859	0.005
58		Precentral gyrus (PrG)	R	A4ul: area 4 (upper limb region)	34, −19, 59	2.369	0.045
68		Paracentral lobule (PCL)	R	A4ll: area 4 (lower limb region)	5, −21, 61	2.658	0.029
102	Temporal lobe	Inferior temporal gyrus (ITG)	R	A20cv: caudoventral of area 20	54, −31, −26	2.628	0.030
124		Posterior superior temporal sulcus (pSTS)	R	cpSTS: caudoposterior superior temporal sulcus	57, −40, 12	2.539	0.035
128	Parietal lobe	Superior parietal lobule (SPL)	R	A7c: caudal area 7	19, −69, 54	3.112	0.014
130		Superior parietal lobule (SPL)	R	A5l: lateral area 5	35, −42, 54	3.164	0.013
136		Inferior parietal lobule (IPL)	R	A39c: caudal area 39 (PGp)	45, −71, 20	2.474	0.038
140		Inferior parietal lobule (IPL)	R	A40rd: rostrodorsal area 40 (PFt)	47, −35, 45	3.157	0.013
144		Inferior parietal lobule (IPL)	R	A39rv: rostroventral area 39 (PGa)	53, −54, 25	2.770	0.024
146		Inferior parietal lobule (IPL)	R	A40rv: rostroventral area 40 (PFop)	55, −26, 26	2.632	0.030
151		Precuneus (Pcun)	L	dmPOS: dorsomedial parietooccipital sulcus (PEr)	−12, −67, 25	2.475	0.038
152		Precuneus (Pcun)	R	dmPOS: dorsomedial parietooccipital sulcus (PEr)	16, −64, 25	2.731	0.026
154		Precuneus (Pcun)	L	A31: area 31 (Lc1)	6, −54, 35	2.404	0.043
158		Postcentral gyrus (PoG)	R	A1/2/3tonla: area 1/2/3 (tongue and larynx region)	56, −10, 15	2.387	0.044
192	Occipital lobe	Medioventral occipital cortex (MVOcC)	R	rCunG: rostral cuneus gyrus	7, −76, 11	3.177	0.013
198		Medioventral occipital cortex (MVOcC)	R	vmPOS: ventromedial parietooccipital sulcus	15, −63, 12	2.441	0.041
199		Lateral occipital cortex (LOcC)	L	mOccG: middle occipital gyrus	−31, −89, 11	2.329	0.048
200		Lateral occipital cortex (LOcC)	R	mOccG: middle occipital gyrus	34, −86, 11	2.716	0.026
202		Lateral occipital cortex (LOcC)	R	V5/MT+: area V5/MT+	48, −70, −1	3.025	0.016
205		Lateral occipital cortex (LOcC)	L	iOccG: inferior occipital gyrus	−30, −88, −12	2.914	0.019
208		Lateral occipital cortex (LOcC)	R	msOccG: medial superior occipital gyrus	16, −85, 34	2.550	0.034
236	Subcortical nuclei	Thalamus (Tha)	R	Stha: sensory thalamus	18, −22, 3	2.674	0.028

*, the significance threshold was set at 0.05. ROI, region of interest; GMV, gray matter volume; PD, Parkinson's disease; MRgFUS, magnetic resonance imaging-guided focused ultrasound; MNI, Montreal Neurological Institute.

https://dx.doi.org/10.21037/qims-22-1403

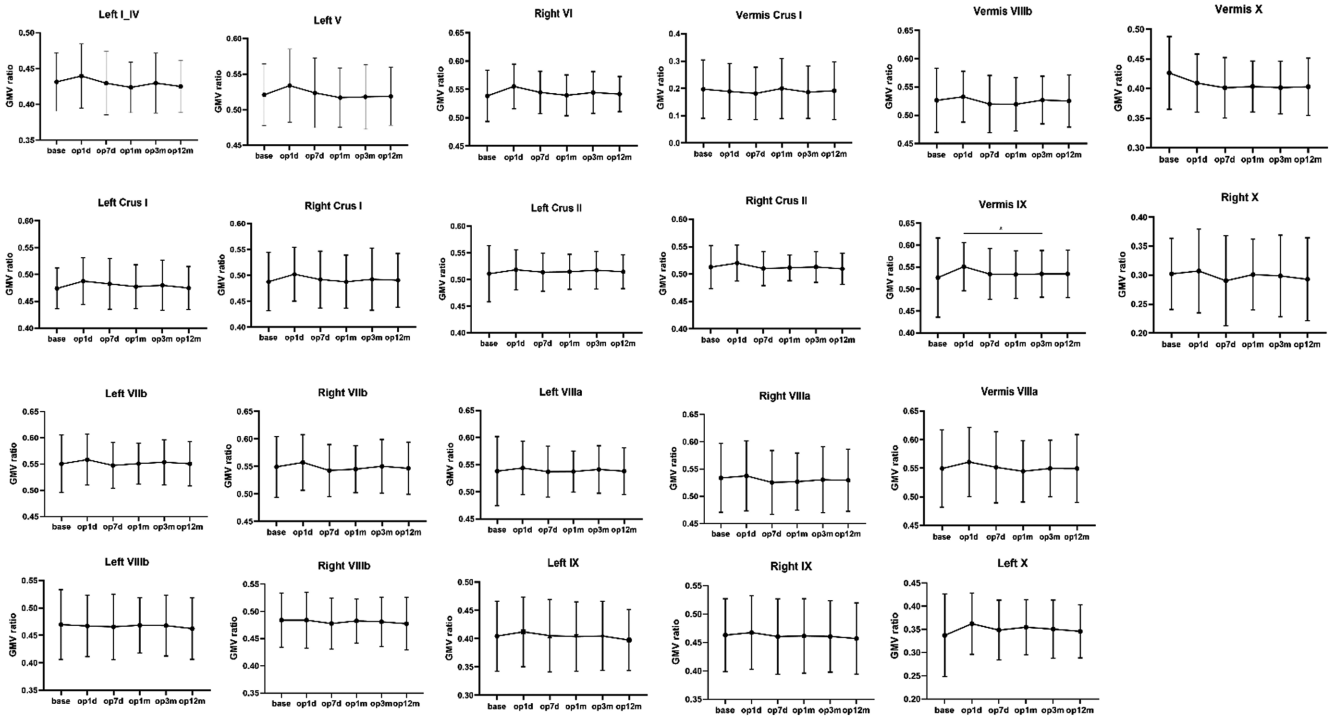

Figure S1 The changing trends in GMV in cerebellar subregions after MRgFUS thalamotomy. GMV, gray matter volume; MRgFUS, magnetic resonance imaging-guided focused ultrasound; op1d, 1 day post-operation; op7d, 7 days post-operation; op1m, 1 month post-operation; op3m, 3 months post-operation; op12m, 12 months post-operation.

https://dx.doi.org/10.21037/qims-22-1403